Investigation of the Effects of Stress Related Genes on *Escherichia coli* Fermentation

by

Michaella Hernandez

A Thesis Presented in Partial Fulfillment
of the Requirements for the Degree
Master of Science

Approved April 2022 by the
Graduate Supervisory Committee:

Xuan Wang, Chair
David Nielsen
Arul Varman

ARIZONA STATE UNIVERSITY

May 2022

ABSTRACT

The current use of non-renewable fossil fuels for industry poses a threat for future generations. Thus, a pivot to renewable sources of energy must be made to secure a sustainable future. One potential option is the utilization of metabolically engineered bacteria to produce value-added chemicals during fermentation. Currently, numerous strains of metabolically engineered *Escherichia coli* have shown great capacity to specialize in the production of high titers of a desired chemical. These metabolic systems, however, are constrained by the biological limits of *E. coli* itself. During fermentation, *E. coli* grows to less than one twentieth of the density that aerobically growing cultures can reach. I hypothesized that this decrease in growth during fermentation is due to cellular stress associated with fermentative growth, likely caused by stress related genes. These genes, including toxin-antitoxin (TA) systems and the *rpoS* mediated general stress response, may have an impact on fermentative growth constraints. Through transcriptional analysis, I identified that the genes *pspC* and *relE* are highly expressed in fermenting strains of both wild type and metabolically engineered *E. coli*. Fermentation of toxin gene knockouts of *E. coli* BW25113 revealed their potential impacts on *E. coli* fermentation. The inactivation of *ydcB, lar, relE, hipA, yjfE, chpA, ygiU, ygjN, ygfX, yeeV, yjdO, yjgK* and *ydcX* did not lead to significant changes in cell growth when tested using sealed tubes under microaerobic conditions. In contrast, inactivation of *pspC, yafQ, yhaV, yfjG* and *yoeB* increased cell growth after 12 hours while inactivation *yncN* significantly arrested cell growth in both tube and fermentation tests, thus proving these toxins' roles in fermentative growth. Moreover, inactivation of *rpoS* also significantly

hindered the ability of *E. coli* to ferment, suggesting its important role in *E. coli* fermentation.

ACKNOWLEDGMENTS

I would first like to thank Dr. Xuan Wang for the opportunity to work in his lab. His mentorship and wisdom have been paramount in not only guiding my research but also achieving my personal goals. I would also like to thank my committee members, Drs. David Nielsen and Arul Varman, for their support in my academic pursuits. Additionally, I would like to express my gratitude to all of my fellow lab members for their kindness and willingness to offer help. They have made the Wang lab a truly supportive environment and have always motivated me in my research. Finally, I would especially like to thank my mentor, Rodrigo Martinez, for his continued support, insight, and patience during the entire process of conducting this thesis

TABLE OF CONTENTS

Page

LIST OF TABLES

Table Page

LIST OF FIGURES

CHAPTER 1

INTRODUCTION

1.1 Biological Constraints of Metabolic Engineering

The manufacture of countless goods including pharmaceuticals, animal feedstocks, and food additives rely on the availability of petroleum (Choi et al., 2019; S. H. Park et al., 2014; Piao et al., 2019). The current rate of petroleum consumption for industry poses a threat for future generations as this nonrenewable resource continues to diminish (Chen et al., 2021). While fossil fuels are essential to industry as we know it, there are a number of drawbacks to utilizing them as a sole source of energy. Their destruction has been noted in spills disrupting marine ecosystems and in global climate changes (Kallio et al., 2021; Marcus, 2021). Thus, pivoting to biobased fuels for industrial chemical synthesis is becoming an increasingly attractive option as they can be synthesized from renewable carbon sources (Ganesh et al., 2015). Metabolically engineered *Escherichia coli* strains have been developed to specialize in the production of various value-added chemicals (i.e., malate, succinate, aspartate) during fermentation (Flores et al., 2020; Martinez et al., 2019; Zhang et al., 2011). While these bacteria-derived products have potential to be more sustainable than their petroleum-derived counterparts, these engineered strains must be further optimized to compete with the current industrial demands.

Bioproduction via *E. coli* fermentation is currently limited by several factors. Previous data collected from my lab shows that while *E. coli* can reach an optical density at 550 nanometers (OD_{550nm}) of above 200, anaerobically growing *E. coli* will not exceed an OD_{550nm} of 10. Additionally, my lab found that a rapid decline in cell viability occurs

after two days of fermentation in the ethanol producing strain LY180, and similar observations were made for other production strains. The low maximum OD_{550nm} and loss of viability suggest that there are underlying mechanisms active during anaerobic fermentation that are responsible for inhibiting cell proliferation and decreasing viability. It has been shown that aerobically growing *E. coli* are significantly more resistant to nutritional and osmotic stress than anaerobically growing cultures (King & Ferenci, 2005) which may be an explanation for the differences observed. *E. coli* has developed a number of systems to deal with nutritional and osmotic stress, including toxin-antitoxin (TA) systems and the *rpoS* mediated general stress response. This thesis serves to investigate the potential roles of these stress related genes in *E. coli* fermentation.

1.2 Toxin-Antitoxin Systems in E. coli

One potential bottleneck for growth and biochemical production in engineered stains is the presence of native toxin-antitoxin (TA) systems. There are currently at least 39 toxin genes native to *E. coli* K-12 (Song & Wood, 2020), and the advantage to having each remains poorly understood on a physiological level. The effects of toxins have been somewhat characterized for select strains of *E.coli* growing aerobically (Tsilibaris et al., 2007), but little has been done to study these systems in fermenting *E. coli*. Furthermore, the effects of native toxins on metabolically engineered strains have yet to be explored.

A TA system is usually encoded as an operon with both toxin and antitoxin genes simultaneously expressed. Native *E. coli* toxins are proteins that disrupt cellular functions in a number of ways, often inhibiting metabolism and growth (and on rare occasion, inducing cell death). The presence of the antitoxin, which is less stable than its toxin counterpart, inhibits the effects of the toxin under normal cellular conditions

(Goormaghtigh et al., 2018). If synthesis of the antitoxin is disrupted, the more stable toxin persists freely and in high enough quantity to exhibit its toxic effect on the cell. While toxins must be translated into proteins to function, antitoxins differ in their format with some existing as proteins and others as antisense or noncoding RNAs. The method by which the antitoxin disrupts the toxin differs between TA system types.

Type I TA systems consist of a separately transcribed toxin and antitoxin. Type I toxins typically exhibit toxicity through disruption of the cellular membrane. The type I antitoxin is transcribed as an antisense RNA which binds to the toxin mRNA, thereby inhibiting its translation (Yamaguchi et al., 2011). In a Type II TA system, the toxin and antitoxin are transcribed from the same promoter. Both toxin and antitoxin are translated, and the antitoxin forms a non-toxic complex with the toxin protein. This TA complex acts as a repressor to the TA operon. Under stressed conditions, the antitoxin is degraded by proteases and the toxin is free to perform its function. The degradation of antitoxin also decreases the concentration of TA complexes, leading to derepression of the TA operon and increased expression of the TA genes (Yamaguchi et al., 2011). A Type III TA system consists of a toxin protein that is inhibited by an RNA antitoxin through direct binding (Harms et al., 2018). In a Type IV TA system, the antitoxin is translated into a protein and subsequently binds to its cognate toxin's target. This blocks the toxin from binding and exhibiting its effect on the target (Kedzierska & Hayes, 2016). In a Type V TA system, the antitoxin is translated into an RNase protein specific to the mRNA of its cognate toxin. The toxin mRNA is then cleaved in the presence of antitoxin protein, effectively blocking translation of the toxin (Wang et al., 2012, 2013). To guide the search for toxin genes relevant to this study, all reported toxin encoding genes in the

EcoCyc database (Keseler et al., 2011) present in *E. coli* W (ATCC 8739) were compiled into a table (Table 1).

The abundance and prevalence of chromosomal TA systems in *E. coli* suggest there may be some benefit to the host despite the potentially lethal effects of toxins. Current literature highlights the role of TA systems in plasmid addiction, where plasmids encode TA systems to ensure their own uptake in the host (Díaz-Orejas et al., 2017; Kroll et al., 2010). Cells that maintain the plasmid also maintain the ability to express an antitoxin and mitigate the cognate toxin's effects. Conversely, cells that lose the plasmid no longer produce antitoxin and are subject to the effects of the stable persisting toxin (Kroll et al., 2010). The plasmid addiction model demonstrates a clear function of the TA systems themselves but does not provide insight into the benefit of retaining the multiple chromosomal TA systems that exist in *E. coli*.

TA systems are often characterized by their role in the formation of persister cells, which allow bacteria to survive harsh environments by reducing their metabolism or becoming metabolically inactive (Kim & Wood, 2016). When nutrients are scarce or sporadically available, persister cells are able to survive by entering a state of dormancy and conserving their resources (Verstraeten et al., 2015). The ability of TA systems to induce persistence and thus alter metabolism raises the question of whether or not these systems contribute significantly to the growth changes observed in fermenting *E. coli.* While there have been numerous studies linking TA systems to persistence (Hall et al., 2017; Kedzierska & Hayes, 2016; Page & Peti, 2016), there is a lack of convincing evidence that the inactivation of TA systems actually resuscitates persister cells which

has led to controversy in the field (Harms et al., 2017; Song & Wood, 2020). Thus, it is unclear what exact role TA systems have on bacterial growth and persistence.

1.3 The rpoS Mediated Stress Response

While most commonly known as a commensal of the human GI tract, (Gao et al., 2014) *E. coli* is relatively versatile as it can be grown under a multitude of conditions and has even been cultured in space (Zea et al., 2017). One gene that contributes to the versatility of culture conditions that *E. coli* grows in is the master regulator of the general stress response, *rpoS*. The *rpoS* gene encodes the sigma factor, σ^S , which regulates genes associated with sugar metabolism, acid tolerance, and oxidative stress (King & Ferenci, 2005; Schellhorn, 2020). Cells in the exponential growth phase and/or grown in optimal conditions express low levels of σ^S. An accumulation of σ^S occurs when the cells are depleted of nutrients, environmental factors rapidly change, or when cells enter the stationary phase (Schellhorn, 2020). A recent study showed that overexpression of *rpoS* increased propionic acid tolerance in fermenting *E. coli* BL21 (Run & Tian, 2018) , suggesting that *rpoS* could be a key gene in the optimization of metabolically engineered strains that produce high titers of acidic products.

Through the characterization of any detrimental effects that native stress related genes have on *E. coli* fermentation, this research aims to guide the process of optimizing growth and chemical yield in specialized strains. Thus, it was hypothesized that stress related genes play a role in the constraint of fermentative growth.

Table 1. Relevant toxin genes native to *E. coli* W

B number	Toxin	Antitoxin	Type	Function(s)
b4428	*ydcB*	*sokB*	I	forms pores in the cytoplasmic membrane that induce ATP leakage
b1348	*lar*	*ralA*	I	Rac prophage, non-specific DNA endonuclease
b4618	*tisB*	*istR*	I	Forms persister cells, predicted to span the inner membrane
b4225	*yjfE*	*chpS*	II	Inhibits cell growth through RNA cleavage
b4532	*yncN*	*hicB*	II	Cleaves mRNAs and inhibits growth (after nutrient starvation)
b3083	*ygjN*	*ygjM*	II	Cleaves coding regions of translated mRNAs (mRNA interferase)
b1507	*hipA*	*hipB*	II	Mediates persister cell formation and can induce growth arrest
b2782	*chpA*	*chpR*	II	Inhibits translation inhibition through sequence specific ribonuclease activity, causes programmed cell death response
b3022	*ygiU*	*ygiT*	II	Reversible growth inhibitor and mRNA interferase, causes cell elongation
b1306	*pspC*	*pspB*	II	Regulator of *psp* operon in response to phage infection, overexpression inhibits cell growth (putative TA system)
b2619	*yfjG*	*yfjF*	II	Inhibits initiation of translation and cell growth (putative TA system)
b1563	*relE*	*relB*	II	Causes reversible inhibition of cell growth through translation inhibition
b0225	*yafQ*	*dinJ*	II	Inhibits translation through mRNA cleavage at AAA codons
b3130	*yhaV*	*prlF*	II	Ribosome dependent ribonuclease (mRNA interferase)
b4539	*yoeB*	*yefM*	II	Inhibits translation initiation through mRNA cleavage
b2005	*yeeV*	*yeeU*	IV	Inhibits GTPase activity and polymerization of cell division proteins, FtsZ and MreB
b2896	*ygfX*	*ygfY*	IV	Inhibits polymerization of FtsZ and MreB
b0245	*ykfI*	*yafW*	IV	Inhibits cell growth under ectopic expression (Brown & Shaw, 2003)
b4559	*yjdO*	*yjdK*	V	Disrupts cell membrane potential and reduces ATP levels
b1445	*ydcX*	N/A	N/A	Damages the cell membrane and reduces ATP levels, referred to as an “orphan toxin” (has no known antitoxin)
b4252	*yjgK*	N/A	N/A	TA biofilm protein, combined TA deletions increase expression of this protein

Canonical (non-hypothetical) and putative toxins native to *E. coli* W were included in this table. B numbers are listed for toxin genes and antitoxins are listed after their cognate toxin. All data was obtained from the EcoCyc database (Keseler et al., 2011) unless otherwise indicated.

CHAPTER 2

RESULTS

2.1 Transcriptional Analysis of Stress Related Genes

Previous fermentations of wild type *E. coli* Crooks (ATCC 8739) and two ethanol producing strains (KO11 and LY180) were transcriptionally analyzed for quantification of gene expression. Briefly, mRNA transcripts were converted to cDNA via reverse transcription and then analyzed using DNA microarray by NimbleGen (Madison, WI). The resulting fluorescence signal was Log_2 transformed to obtain a numerical value for expression. To determine which stress related genes had above average expression, the expression values of all native *E. coli* genes from the aforementioned samples were averaged and compared to the expression of each previously identified toxin encoding gene (Table 1) as well as *rpoS*. Across the three strains, groupings of below average, average, and above average expression levels were identified. Toxin genes, *pspC,* and *relE* were consistently expressed at levels above average while toxin genes *lar, ygjN, yeeU/V,* and *ydcX* were expressed at levels below average. While most relative transcription levels remained consistent between all strains, *yjfE, chpS,* and *yefM* were expressed at higher levels in both engineered strains than in the wild type. Additionally, the *ygiU/T* system was more highly expressed in the wild type strain than in both engineered strains.

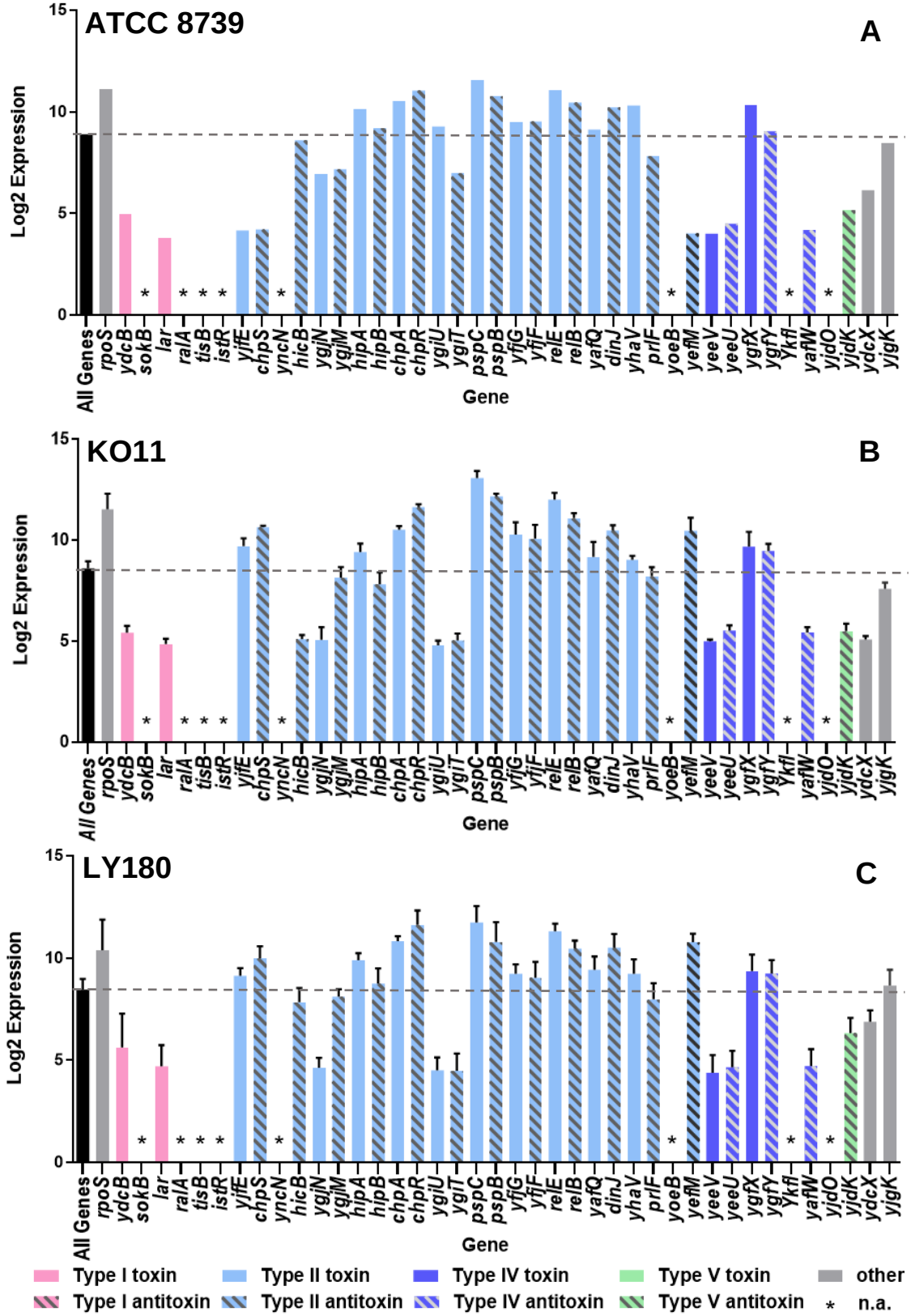
ATCC 8739
A
KO11
B
LY180
C
Log2 Expression
Gene
All Genes
rpoS
ydcB
sokB
lar
ralA
tisB
istR
yifE
chpS
yncN
hicB
ygiN
ygiM
hipA
hipB
chpA
chpR
ygiU
ygiT
pspC
pspB
yfiG
yfjF
relE
relB
yafQ
dinJ
yhaV
prlF
yoeB
yefM
yeeV
yeeU
ygfX
ygfY
Ykfl
yafW
yjdO
yjdK
ydcX
yjgK
Type I toxin
Type I antitoxin
Type II toxin
Type II antitoxin
Type IV toxin
Type IV antitoxin
Type V toxin
Type V antitoxin
other
n.a.

Figure 1. Log_2 transformed expression of stress related genes native to *E. coli*. Gene expression is plotted against the average expression of all genes in *E. coli* with the dotted line indicating average expression. Toxins (solid bars) are plotted to the left of their cognate antitoxin (striped bars). (A) Gene expression in ATCC 8739. Genes *rpoS* and, *pspC* are expressed at significantly higher than average levels while *ydcB, lar, yjfE, chpS, yefM, yeeV, yeeU, yafW, yjdK* and *ydcX* are expressed at levels significantly below average. Expression of toxin genes *hipA, ygiU, pspC, relE, yhaV*, and *ygfX* was higher than that of their cognate antitoxins. (B) Gene expression in KO11. Higher than average expression was observed in, *pspC, pspB, relE, relB,* and *chpR.* Below average expression was observed in *ydcB lar, hicB, ygiN, ygiU/T, yeeU/V, yafW, yjdK,* and *ydcX*. (C) Gene expression in LY180. Similar trends appear with *pspC, chpR,* and *relE* expressed at above average levels and *lar, ygiN, ygiU/T, yeeU/V,* and *yafW* expressed at below average levels.

2.2 Microaerobic Growth Tests of Toxin Gene Knockouts

To test which of the previously identified toxin genes may contribute to changes in fermentative growth, 36-hour microaerobic growth tests were utilized as a proxy for microaerobic/anaerobic fermentative growth performance. Single gene knockout strains obtained from the KEIO collection (Baba et al., 2006) were utilized for all growth tests. Strains were grown for 36 hours and OD_{550nm} was measured every 12 hours (Fig. 2). Relative growth was calculated by normalizing growth of all samples to their respective wild type control. After 12 hours, significant decreases in relative growth were observed in knockouts of *yncN* and *relE* while significant increases were observed in knockouts of *pspC, yafQ, yfjG,* and *yoeB.* Interestingly, all toxin gene knockouts resulting in significant growth alterations were type II toxins. After the 24- and 36-hour time points, most knockout strains-maintained growth consistent with the wild type strain except for the *yncN* knockout strain, which grew to a lower OD_{550nm} than the wild type at all time points. Growth curves can be found in Appendix A (Fig. S1).

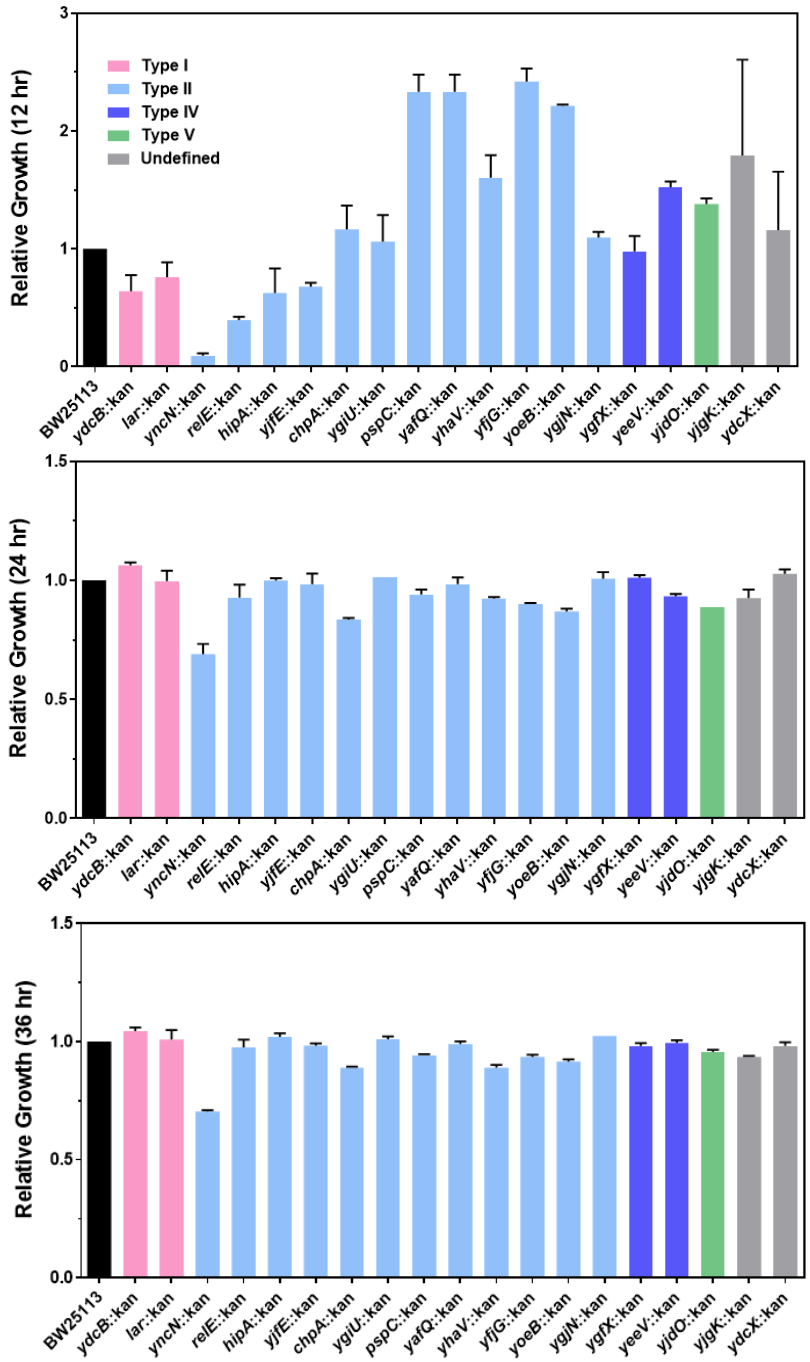

Figure 2. Relative growth of single toxin knockout strains of BW25113 as compared to wild type over 12-hour increments in a microaerobic environment. Samples were normalized to their control and error bars were plotted as the average of at least two biological replicates per strain. Bar color indicates toxin type. Slight decreases in growth were observed in *yncN*, *yoeB*, *yfjG*, *yjdO*, and *chpA* knockouts while all other knockout strains were comparable to the control.

2.3 Fermentation Tests of Selected Single Gene Knockouts

Toxins that were identified to be of interest based on preliminary microaerobic growth testing and transcriptional analysis were chosen for further study in pH and temperature-controlled fermentation vessels (300 mL). Strains of BW25113 with single gene knockouts of *chpA* and *ydcB* were fermented for 120 hours in AM1 media and OD_{550nm} was measured every 24 hours (Fig. 3). Both knockout strains reached their maximum OD_{550nm} after only 24 hours of growth while the wild type reached its maximum OD_{550nm} after 48 hours of growth (Fig. 3A). On average, the *chpA* knockout produced slightly more lactate than the wild type strain and the *ydcB* knockout strain (Fig. 3C, D). Additionally, succinate production was detected in the *chpA* knockout strain but not in any other strain (Fig. 3E).

Next, strains of *E. coli* BW25113 with single knockouts of *pspC*, *ydcB,* and *yhaV* were fermented for 30 hours in AM1 minimal media (Fig. 4). OD_{550nm} was measured over 6- or 12- hour increments. All strains reached their maximum OD_{550} (~2.7) after 19 hours of growth (Fig. 4A) and utilized nearly identical amounts (~14 mL) of base (Fig. 4B). All strains produced similar amounts of lactate and ethanol (Fig. 4C, D).

Single knockouts of *yjdO,* and *yjgK* were also fermented in AM1 minimal media for 36 hours where OD_{550nm} was measured in 6-hour increments (Fig. 5). All knockout strains grew to a similar maximum OD_{550} (~4.2) after 24 hours, with the control strain reaching its maximum OD_{550nm} (~4.3) after 36 hours (Fig. 5A). All strains but BW25113 *yjdO*::kan utilized ~26 mL of base for product neutralization, with the aforementioned strain using ~30 mL (Fig. 5B). All strains produced similar amounts of lactate and

ethanol except *yjdO*::kan which showed slight increases in both metabolite products at 24 hours (Fig. 5C, D).

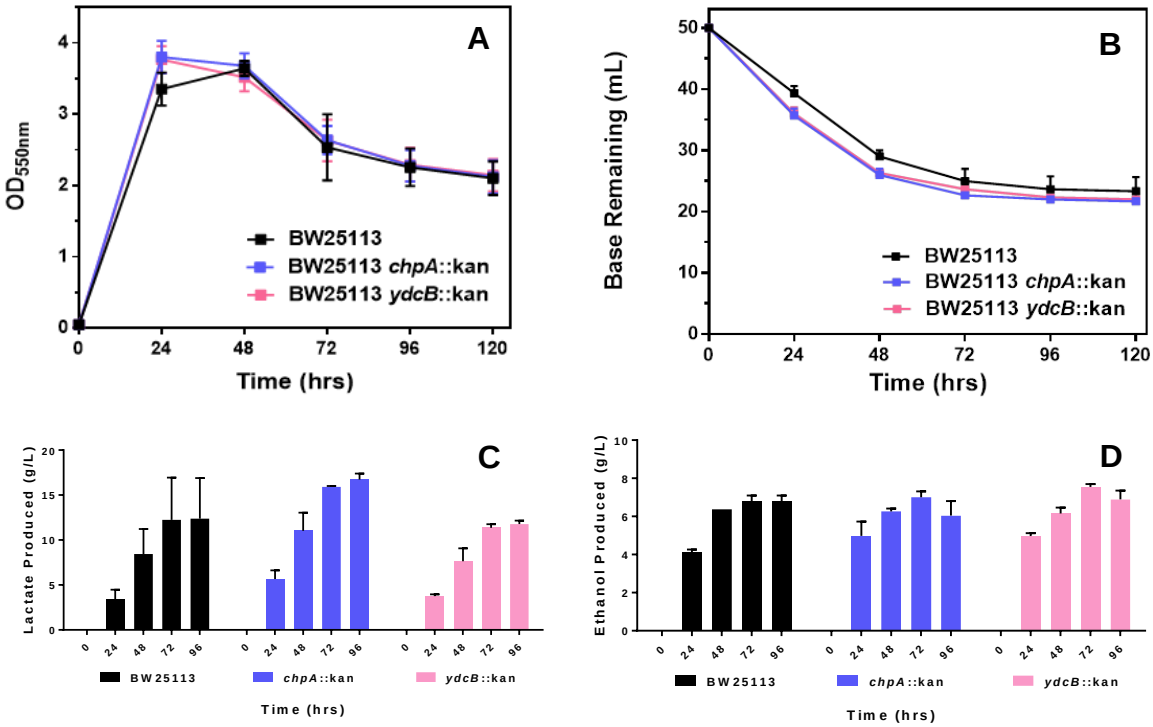

Figure 3. Fermentation of *chpA* and *ydcB* knockouts over 120 hours. (A) Points were plotted as the average of at least two biological replicates per strain. Both *chpA* and *ydcB* deletion strains reached their maximum OD_{550nm} after 24 hours while the control reached maximum OD_{550nm} after 48 hours. Growth remained identical between all strains at all subsequent time points. (B) All strains required ~25 mL of base (6M KOH) to neutralize fermentation products and maintain a pH of 7.0. All strains utilized base at a comparable rate. (C) Average g/L of lactate produced during fermentation. The *ydcB*::kan strain produced fewer grams per liter of lactate than *chpA*::kan, which was comparable to the background strain. (D) Average g/L of ethanol produced during fermentation. All strains produced nearly identical quantities of ethanol at all time points.

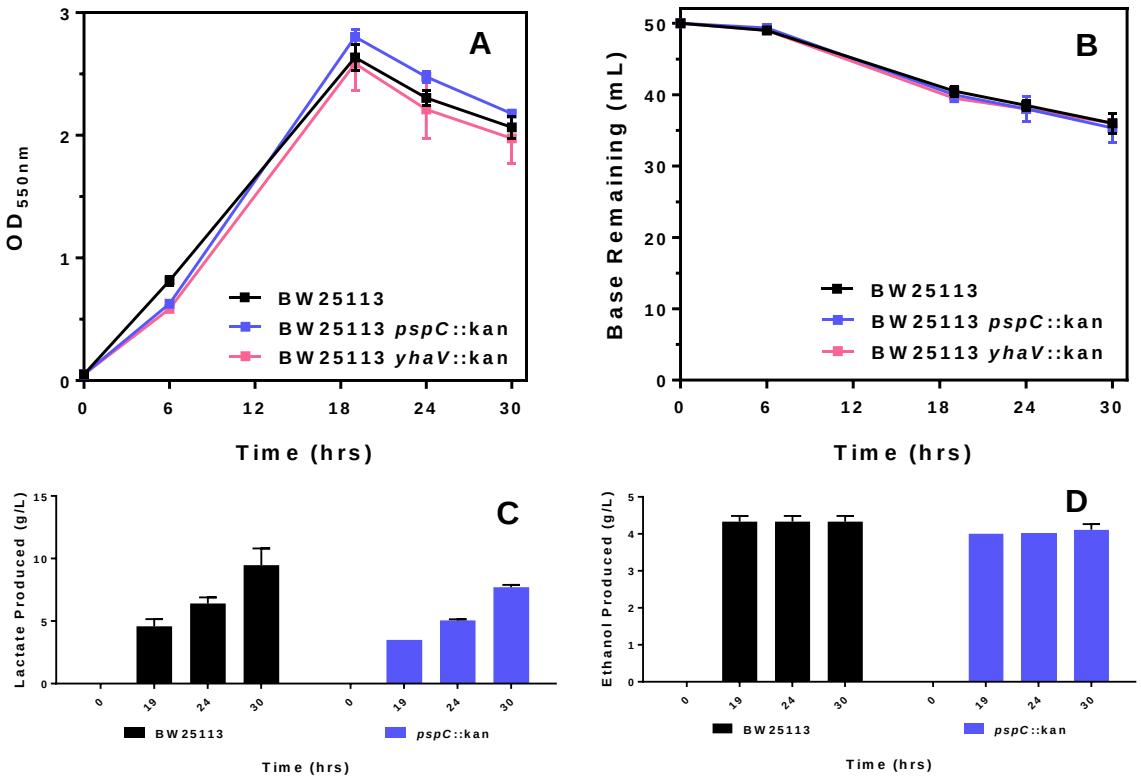

Figure 4. Fermentation of *pspC* and *yhaV* knockouts over 30 hours. (A) Points were plotted as the average of at least two biological replicates per strain. Both knockout strains reached their maximum OD_{550nm} after 19 hours of growth. No significant changes in growth were observed. (B) All strains required ~14 mL of base to neutralize fermentation products and maintain a pH of 7.0 with no significant variation. (C) Average g/L of lactate produced during fermentation. Lactate production by the *yhaV* knockout strain was not measured. Both strains produced similar amounts of lactate during the fermentation. (D) Average g/L of ethanol produced during fermentation. Ethanol production by the *yhaV* knockout strain was not measured. Both strains produced similar amounts of ethanol during the fermentation.

Single knockouts of *yoeB* and *yfjG* were fermented for 42 hours in AM1 minimal media where OD_{550nm} was measured in either 6- or 12-hour increments (Fig. 6). Knockout of *yfjG* resulted in increased growth at all time points after 18 hours while knockout of *yoeB* had no effect on growth (Fig. 6A). Both the *yfjG* and *yoeB* knockout utilized more base than the wild type strain (Fig. 6B) which was consistent with lactate production at the later stages of growth. After 42 hours of growth, both knockout strains

produced increased amounts of lactate, while their ethanol production remained consistent with the control (Fig. 6C, D).

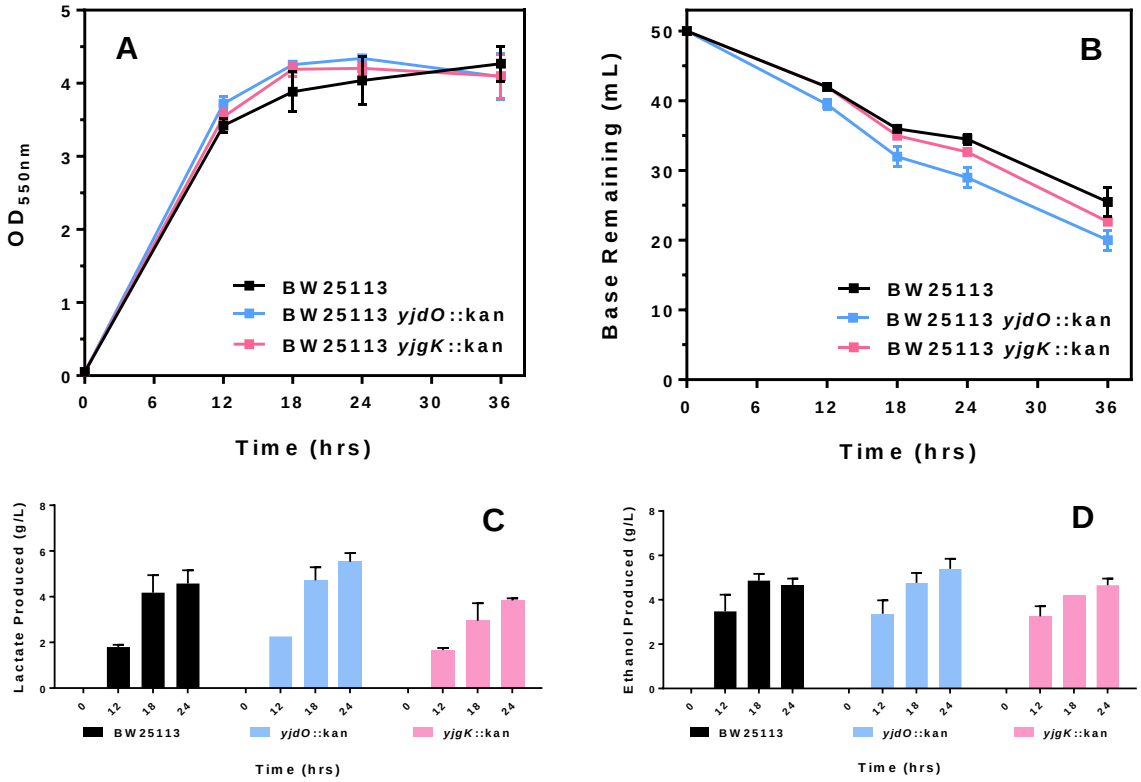

Figure 5. Fermentation of *yjdO*, and *yjgK* knockouts over 36 hours. (A) Growth as measured by OD_{550nm}. Points were plotted as the average of at least two biological replicates. Growth remained consistent between all strains at all time points. (B) Knockout of *yjdO* resulted in a slight increase in base consumption at all time points with all other strains matching the wild type. (C) Average g/L of lactate produced during fermentation. All strains produced similar amounts of lactate, however the *yjdO* knockout produced slightly more after 24 hours. (D) Average g/L of ethanol produced during fermentation. All strains produced similar amounts of ethanol, however the *yjdO* knockout produced slightly more after 24 hours.

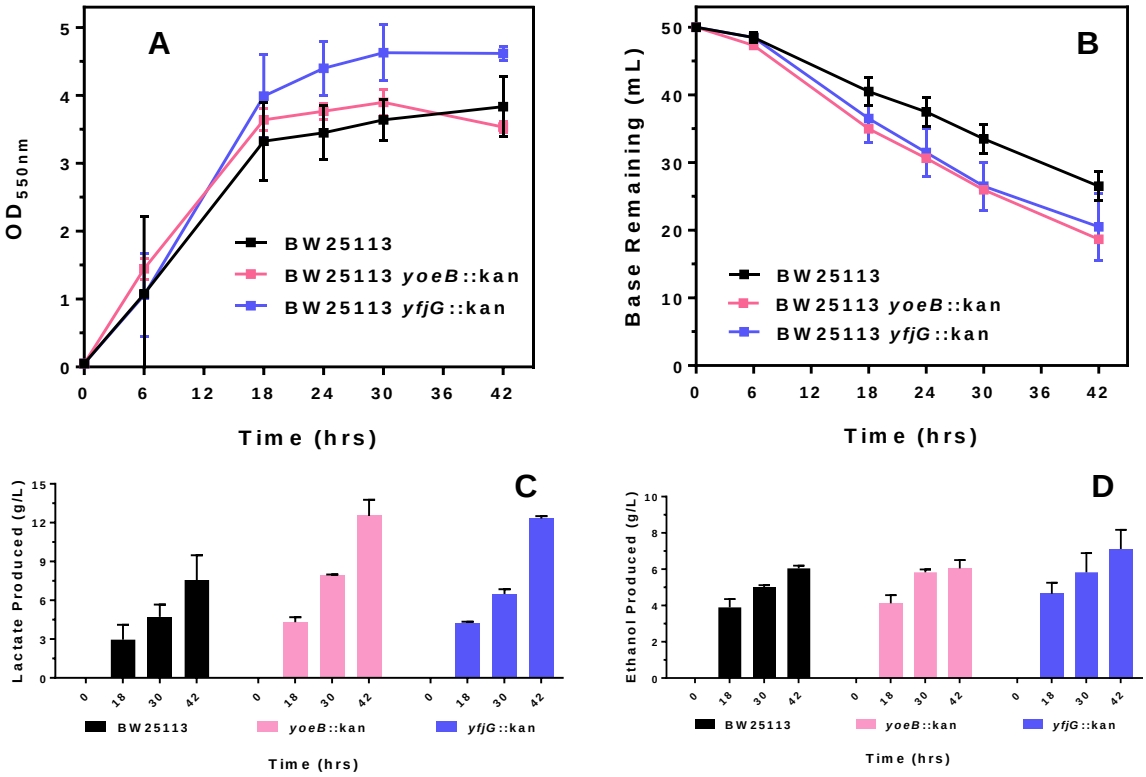

Figure 6. Fermentation of *yoeB* and *yfjG* knockouts over 42 hours. (A) Growth was measured in 6- or 12-hour increments and plotted as the average of at least two biological replicates. Knockout of *yfjG* resulted in increased OD_{550nm} at all time points after 18 hours while knockout of *yoeB* resulted in no change. (B) Average base consumption of both knockout strains was slightly increased at all time points. (C) Average g/L of lactate produced was comparable for all strains at the 18-hour time point. Lactate production was increased in the *yoeB* knockout strain after 30 hours of growth. Lactate production also improved after 42 hours in both knockouts. (D) Average g/L of ethanol produced was similar for all strains at all time points.

A single knockout strain of *yncN* was fermented for 42 hours in AM1 minimal media and OD_{550nm} was measured in 6- or 12-hour increments (Fig. 7). Consistent with tube test results, knockout of *yncN* drastically hindered growth at all time points after 6 hours (Fig. 7A) and base consumption was significantly decreased (Fig. 7B). Both lactate (Fig. 7C) and ethanol production (Fig. 7D) were decreased in the *yncN* knockout strain for all recorded time points.

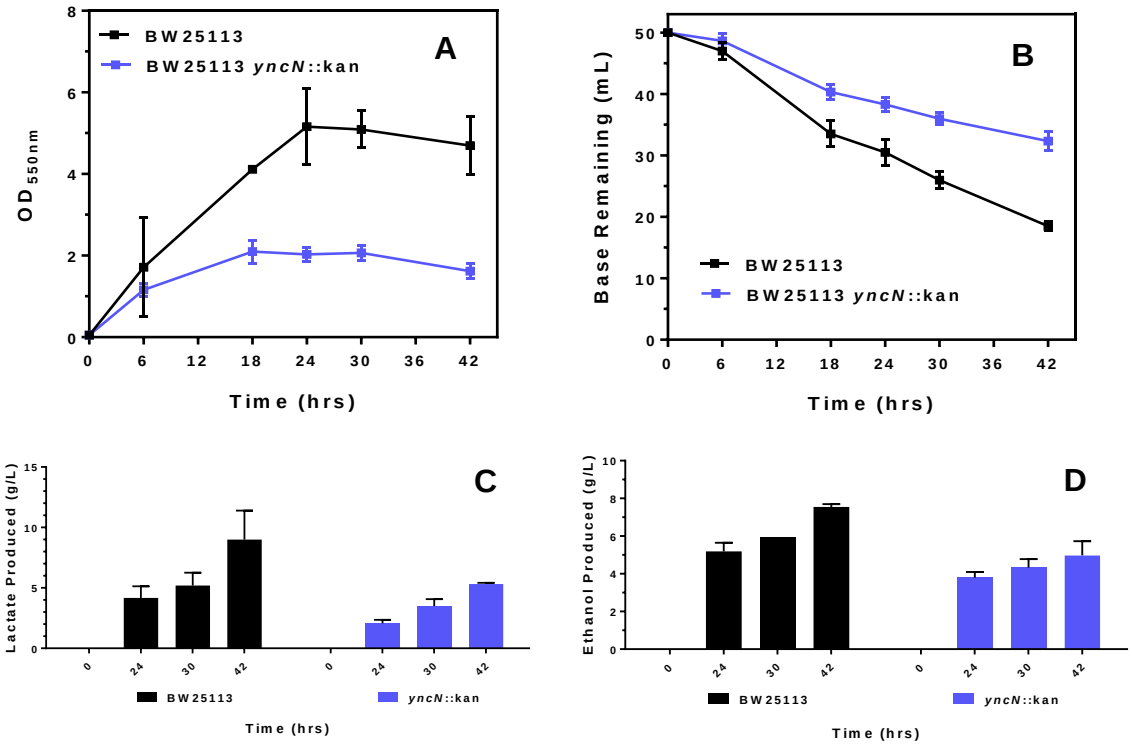

Figure 7. Fermentation of *yncN* knockout over 42 hours. (A) Growth rate was measured in 6- or 12- hour increments and plotted as the average of at least two biological replicates. Knockout of *yncN* resulted in significantly decreased growth for all time points after 18 hours. (B) Average base consumption of the *yncN* knockout strain was significantly decreased at all time points after 18 hours. This is consistent with both (C) lactate and (D) ethanol production, which were both decreased at all time points in the knockout strain.

Finally, an *rpoS* knockout strain was fermented for 72 hours in AM1 minimal media and OD_{550nm} was measured every 24 hours (Fig. 8). Knockout of *rpoS* resulted in significantly decreased growth at all time points (Fig. 8A) but similar base consumption was observed (Fig. 8B). Lactate production was significantly decreased after 72 hours (Fig. 8C) while ethanol production remained nearly identical to the control (Fig. 8D). Two genes regulated by *rpoS*, *katE* and *katG*, are involved in mitigating oxidative stress. A double knockout strain of catalase encoding genes *katE* and *katG* was also fermented with no significant changes in growth (Fig. S2).

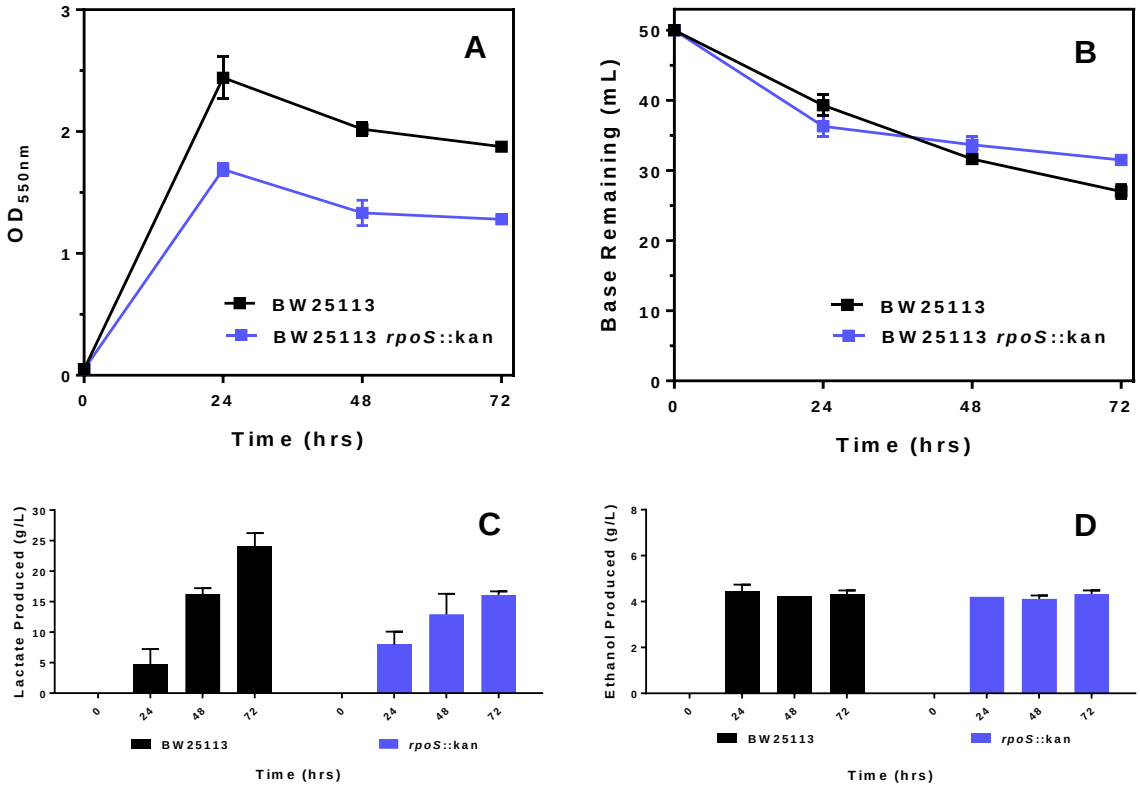

Figure 8. Fermentation of *rpoS* knockout over 72 hours. (A) OD_{550nm} was measured every 24 hours. Points were plotted as the average of three biological replicates. Knockout of *rpoS* resulted in a significant decrease in growth at all time points. (B) Knockout of *rpoS* did not significantly alter base consumption. (C) The *rpoS* knockout strain produced less lactate after 48 hours and (D) no change was noted in ethanol production.

CHAPTER 3

DISCUSSION

3.1 Effects of Stress Related Genes on Fermentation

Metabolic engineering of microbes for renewable production is a potential solution to the problems associated with dependence on petroleum as a major source of energy. Previous research has shown promising outcomes in the development of highly specialized chemical producing strains of *E. coli*. However, these strains must be fermented to obtain the desired end products (succinate, aspartate, malate, etc.) which introduces limitations to culture density and growth. The mechanism for this change in growth between aerobically and anaerobically grown cultures remains poorly understood, thus native TA systems and stress related genes may provide some insight into the underlying factors that contribute to these differences.

To study the effects of toxins on fermentation, all reported and confirmed toxin genes present in the EcoCyc database (Keseler et al., 2011) in *Escherichia coli* W were compiled in Table 1. *E. coli* W has widespread use in industrial microbiology laboratories for biochemical production (Noh et al., 2018; Novak et al., 2018; J. H. Park et al., 2011) and has been engineered to produce a variety of chemicals including ethanol, lactic acid, and alanine (Archer et al., 2011). *E. coli* W was identified by this study to have 21 confirmed and putative toxin genes. Thus, this strain was chosen as it exhibits relevance to the pursuit of strain optimization in bioproduction. This approach to toxin identification is limited, as genes that are not reported in the EcoCyc database (Keseler et al., 2011) and genes not listed as toxins in the database are not identifiable and were consequently excluded from this study.

To determine genes likely to have a significant impact on fermentation, previous transcriptional profiles obtained from fermenting cultures were investigated (Fig. 1). There were several genes identified to have similar expression across all strains. Genes that were consistently expressed at below average levels included *lar*, *ygjN*, and *yeeU/V*. Genes that were expressed at above average levels across all three strains include *pspC*, and *relE*. Interestingly, all of the highly expressed genes encode toxins belonging to a Type II TA system. As such, each of these genes are encoded with their cognate antitoxin in an operon and consequently, it is expected that there would be similar expression of both toxin and antitoxin since they are regulated by the same promoter. Transcriptional data shows that the ratio of toxin to antitoxin transcripts for the type II systems including *hipA, chpA, pspC,* and *relE* is not 1:1. Toxin transcript abundance is higher than that of the antitoxin in the *hipA, pspC,* and *relE* systems, while the opposite is observed in the *chpA* and *yafQ* systems. This data suggests that there should be some level of toxicity associated with the presence of *hipA, pspC,* and *relE*, as their antitoxins are likely subject to degradation during fermentation. This was explored further through fermentation of the BW25113 *pspC* knockout strain.

The phage shock protein (Psp) system is active as a stress response to heat, osmotic shock, and phage infection (Brissette et al., 1991). This system also functions to maintain the bacterial cell envelope and becomes ineffective when the cell envelope is damaged (Wu et al., 2018). Though transcriptional data shows *pspB/C* expression as above average, the level of toxicity exhibited by *pspC* is not a significant factor affecting culture growth or inhibiting the ability of the cell to produce metabolites (Fig. 4). Thus, the type of stress that induces the *psp* operon is likely not relevant to fermentation.

Microaerobic growth tests were utilized as a screening tool and served as a proxy for 300 mL fermentation tests (Fig. 2). These tests were conducted in sealed 45 mL glass screw cap tubes and lacked the necessary hardware for dispensing base to automatically adjust pH. To mitigate pH changes, MOPS buffer was included in the growth test media. Growth tests were also limited to 36 hours due to potential experimental discrepancies caused by low pH, and the first time point (12 hours of growth) was used to determine candidate strains for 300 mL fermentations.

Knockout of *yncN* (commonly referred to as *hicA*) significantly reduced growth and metabolite production during fermentation (Fig. 7). The toxin protein HicA induces cleavage of mRNA and is classified as an mRNA interferase (Butt et al., 2014). When the *hicAB* TA pair was first identified, it was initially hypothesized that *hicA* was the antitoxin (Yamaguchi & Inouye, 2011). This is due to the presence of a partial RNase H fold that was found in the structure of the HicB protein (Manav et al., 2019). RNase H folds are present in a variety of enzymes involved in diverse processes including replication, recombination, and CRISPR-Cas immunity. More interestingly, RNase H folds have also been found in enzymes involved in RNA interference (RNAi) (Moelling et al., 2017). The phenotypical changes observed in the *yncN* knockout may be attributed to RNAi activity of the HicB antitoxin, which is downstream of the deleted toxin gene and remains active. Additionally, the KEIO collection knockouts were generated by replacing the native gene with a kanamycin resistance cassette. The presence of this cassette may influence regulation of the antitoxin and potentially exacerbate any harmful effects. Alternatively, there may be some underlying mechanism by which the YncN

protein is somehow beneficial to fermentation. While this explanation is not well supported by current literature, it cannot yet be ruled out with certainty.

In Figure 8, it was shown that knockout of *rpoS* significantly hindered growth and lactate production. This result indicates that genes regulated under the general stress response have some beneficial effect on fermentation. The general stress response is most commonly associated with changes in pH, osmolarity, temperature, or nutrient availability (Battesti et al., 2011). Batch fermentations in this study were conducted at a constant temperature and pH with 100 g/L of glucose present in the media. If the general stress response is active under these conditions, it is likely that the cells are primarily experiencing osmotic stress. This may be somewhat mitigated by altering the fermentation media, however stress due to high osmolarity becomes a significant issue for engineered strains producing high titers of extracellular metabolites.

3.2 Future Directions

Investigation into the potential role of the antitoxin *hicB* in RNAi could provide insight into the growth defects observed in the *yncN* knockout strain. If fermentation of a *yncN/hicB* double knockout results in the restoration of normal growth, it is likely that unbound HicB has off target activity or is otherwise implicated in some form of RNAi. Additionally, overexpression of *yncN* could clarify whether or not the YncN toxin protein plays a beneficial role in fermentation. Overexpression of *rpoS* may also provide insight into the potential benefit of the genes regulated under the general stress response and their role in fermentation.

Knockout of individual toxin genes in the BW25113 background has provided informative preliminary data. However, testing the effects of toxin deletions in

engineered chemical-producing strains will better reveal the potential for TA systems to be used in strain optimization. Strains BW25113 *yoeB::*kan and BW25113 *yfjG::*kan both had increased lactate production during fermentation. Deletion of these genes in a lactate producing strain, like TG114 (Grabar et al., 2006), could help reveal the extent to which toxin gene deletion may enhance chemical production.

CHAPTER 4

MATERIALS AND METHODS

4.1 Transcriptional Analysis

Transcriptional data was previously collected by my lab. Briefly, *E. coli* strains ATCC 8739, KO11, and LY180 were fermented and culture samples were collected at the late log phase of growth. Reverse transcription was then utilized to convert mRNA transcripts of all native genes into cDNA. The cDNA fragments were then quantified using DNA microarray and their fluorescence signal was Log_2 transformed to obtain a value for relative transcription. Average expression of all genes was calculated by determining the mathematical average of all gene expression values reported in the study (4237 total).

4.2 Strains, Media, and Growth Conditions

All strains used for growth tests and fermentations are listed in Table S2. and KEIO collection strains were provided courtesy of Dr. David Nielsen. Wild type *E. coli* K-12 BW25113 was used as a control for all growth tests and fermentations. Briefly, the KEIO collection is a library of single gene replacements for genes present in the *Escherichia coli* K-12 BW25113 background. Genes are replaced with a kanamycin resistance cassette flanked by two FRT sites for streamlined deletion.

Prior to fermentations and microaerobic growth tests, samples were first streaked on AM1 minimal media plates (2% glucose [w/v], 100 mM MOPS), placed in an airtight canister, and ventilated with argon gas for 5 minutes before fastening the hermetic seal. Plates were grown at 37°C until colonies were visible (approximately 24 hours).

For microaerobic growth tests, seed cultures were grown in sealed 50 mL conical vials and 25 mL of seed culture media (1X AM1, 2% glucose [w/v], 100 mM MOPS) were inoculated with 5-6 bacterial colonies. Seed cultures were grown for ~16 hours at 30°C in a shaking incubator (120 rpm) and appropriate volumes were transferred to 45 mL of growth test media (1X AM1, 10% glucose [w/v], 100 mM MOPS) to reach an initial OD_{550nm} of 0.01. Growth tests were conducted in 45 mL glass tubes with screw cap seals and left at 37°C. and tubes were inverted three times daily. Growth test tubes were ventilated with argon gas and resealed after each measurement.

For fermentations, 100 mL of seed culture media (as previously mentioned) were inoculated with 5-6 bacterial colonies and grown at 37°C for approximately 16 hours in a shaking incubator (120 rpm). Cultures were centrifuged at 7000 rpm for 5 minutes and pellets were resuspended in 300 mL of fermentation media (1X AM1, 10% glucose w/v) to reach an initial OD_{550nm} of 0.05. Fermentations were conducted in sealed 500 mL jars, grown at 37°C, and maintained at pH of 7.0 by an automatic base (6M KOH) dispenser.

4.3 Analytical Methods

For microaerobic growth tests, sample OD_{550nm} was measured once every 12 hours. For fermentations, sample OD_{550nm} was measured once every 6 to 12 hours. All OD_{550nm} measurements were made using a UV/Vis spectrophotometer (Beckman Coulter DU-730). All metabolite products were quantified using HPLC (Thermo Fisher Scientific UltiMate 3000, Waltham, MA) with an Aminex HPX-87Hcolumn (Bio-Rad) and 4 mM sulfuric acid as the mobile phase (Sievert et al., 2017).

4.4 Genetic Methods

The *katE, katG* double knockout strain was created by first chemically transforming FLP recombinase encoding plasmid pCP20 into the KEIO knockout strain of *katE* (grown on LB + ampicillin plate at 30°C). One transformed colony was transferred to 5 mL of LB media and grown at 43°C overnight. The overnight culture was diluted (10^{-6}) and 50 µL were plated on LB. Colonies were then patched for ampicillin and kanamycin resistance. Sensitive colonies were confirmed to have lost the kanamycin resistance cassette by colony PCR (Fig. S3) leaving only an FRT site behind.

A PCR generated fragment of the *katG*::kan resistance cassette and the flanking genomic regions (221 bp upstream and 267 bp downstream) was used for homologous recombination in the aforementioned *katE*::FRT strain. The *katE*::FRT strain was chemically transformed with plasmid pKD46 and induced with Super Optimal Broth (SOB) containing 5% (w/v) L-arabinose. Cells were then made electrocompetent (washed three times with ice-cold sterile npH_2O) and electroporated with the *katG*::kan fragment. Electroporated cells were recovered for 4 hours at 37°C and plated on LB + kan at 39°C. Colonies were patched on LB + ampicillin to check for plasmid loss and sensitive colonies were confirmed to have the insert via cPCR (Fig. S3). All primers used are listed in Table S1.

REFERENCES

Archer, C. T., Kim, J. F., Jeong, H., Park, J. H., Vickers, C. E., Lee, S. Y., & Nielsen, L. K. (2011). The genome sequence of *E. coli* W (ATCC 9637): comparative genome analysis and an improved genome-scale reconstruction of *E. coli*. *BMC Genomics*, *12*(9). https://doi.org/10.1186/1471-2164-12-9

Baba, T., Ara, T., Hasegawa, M., Takai, Y., Okumura, Y., Baba, M., Datsenko, K. A., Tomita, M., Wanner, B. L., & Mori, H. (2006). Construction of *Escherichia coli* K-12 in-frame, single-gene knockout mutants: The Keio collection. *Molecular Systems Biology*, *2*(1). https://doi.org/10.1038/msb4100050

Battesti, A., Majdalani, N., & Gottesman, S. (2011). The RpoS-Mediated General Stress Response in *Escherichia coli**. *Annual Review of Microbiology*, *65*, 189–213. https://doi.org/10.1146/annurev-micro-090110-102946

Brissette, J. L., Weiner, L., & Ripmaster, T. L. (1991). Characterization and Sequence of the *Escherichia coli* Stress-induced psp Operon. *Journal of Molecular Biology*, *220*(1), 35–48.

Brown, J. M., & Shaw, K. J. (2003). A Novel Family of *Escherichia coli* Toxin-Antitoxin Gene Pairs. *Journal of Bacteriology*, *185*(22), 6600–6608. https://doi.org/10.1128/JB.185.22.6600-6608.2003

Butt, A., Higman, V. A., Williams, C., Crump, M. P., Hemsley, C. M., Harmer, N., & Titball, R. W. (2014). The HicA toxin from Burkholderia pseudomallei has a role in persister cell formation. *Biochemical Journal*, *459*(2), 333–344. https://doi.org/10.1042/BJ20140073

Chen, Y., Zhang, L., Yang, Y., Pang, B., Xu, W., Duan, G., Jiang, S., & Zhang, K. (2021). Recent Progress on Nanocellulose Aerogels: Preparation, Modification, Composite Fabrication, Applications. *Advanced Materials*, *33*(11). https://doi.org/10.1002/adma.202005569

Choi, K. R., Jang, W. D., Yang, D., Cho, J. S., Park, D., & Lee, S. Y. (2019). Systems Metabolic Engineering Strategies: Integrating Systems and Synthetic Biology with Metabolic Engineering. *Trends in Biotechnology*, *37*(8), 817–837. https://doi.org/10.1016/j.tibtech.2019.01.003

Díaz-Orejas, R., Espinosa, M., & Yeo, C. C. (2017). The importance of the expendable: Toxin-antitoxin genes in plasmids and chromosomes. *Frontiers in Microbiology*, *8*(AUG), 1–7. https://doi.org/10.3389/fmicb.2017.01479

Flores, A. D., Choi, H. G., Martinez, R., Onyeabor, M., Ayla, E. Z., Godar, A., Machas, M., Nielsen, D. R., & Wang, X. (2020). Catabolic Division of Labor Enhances

Production of D-Lactate and Succinate From Glucose-Xylose Mixtures in Engineered *Escherichia coli* Co-culture Systems. *Frontiers in Bioengineering and Biotechnology*, *8*. https://doi.org/10.3389/fbioe.2020.00329

Ganesh, M., Senthamarai, A., Shanmughapriya, S., & Natarajaseenivasan, K. (2015). Effective production of low crystallinity Poly(3-hydroxybutyrate) by recombinant *E. coli* strain JM109 using crude glycerol as sole carbon source. *Bioresource Technology*, *192*, 677–681. https://doi.org/10.1016/j.biortech.2015.06.042

Gao, Y. D., Zhao, Y., & Huang, J. (2014). Metabolic modeling of common *Escherichia coli* strains in human gut microbiome. *BioMed Research International*, *2014*. https://doi.org/10.1155/2014/694967

Goormaghtigh, F., Fraikin, N., Putrinš, M., Hallaert, T., Hauryliuk, V., Garcia-Pino, A., Sjödin, A., Kasvandik, S., Udekwu, K., Tenson, T., Kaldalu, N., & Melderena, L. Van. (2018). Reassessing the Role of Type II Toxin-Antitoxin Systems in Formation of *Escherichia coli* Type II Persister Cells. *MBio*, *9*(3), 1–14.

Grabar, T. B., Zhou, S., Shanmugam, K. T., Yomano, L. P., & Ingram, L. O. (2006). Methylglyoxal bypass identified as source of chiral contamination in L(+) and D(-)-lactate fermentations by recombinant *Escherichia coli*. *Biotechnology Letters*, *28*(19), 1527–1535. https://doi.org/10.1007/s10529-006-9122-7

Hall, A. M., Gollan, B., & Helaine, S. (2017). Toxin–antitoxin systems: reversible toxicity. *Current Opinion in Microbiology*, *36*, 102–110. https://doi.org/10.1016/j.mib.2017.02.003

Harms, A., Brodersen, D. E., Mitarai, N., & Gerdes, K. (2018). Toxins, Targets, and Triggers: An Overview of Toxin-Antitoxin Biology. *Molecular Cell*, *70*(5), 768–784. https://doi.org/10.1016/j.molcel.2018.01.003

Harms, A., Fino, C., Sørensen, M. A., Semsey, S., & Gerdes, K. (2017). Prophages and growth dynamics confound experimental results with antibiotic-tolerant persister cells. *MBio*, *8*(6). https://doi.org/10.1128/mBio.01964-17

Kallio, P., Kugler, A., Pyytövaara, S., Stensjö, K., Allahverdiyeva, Y., Gao, X., Lindblad, P., & Lindberg, P. (2021). Photoautotrophic production of renewable ethylene by engineered cyanobacteria: Steering the cell metabolism towards biotechnological use. *Physiologia Plantarum*, *173*(2), 579–590. https://doi.org/10.1111/ppl.13430

Kedzierska, B., & Hayes, F. (2016). Emerging roles of toxin-antitoxin modules in bacterial pathogenesis. *Molecules*, *21*(6), 790. https://doi.org/10.3390/molecules21060790

Keseler *et al.*, *Nuc Acids Res,* 39:D583–90 2011.

Kim, J.-S., & Wood, T. K. (2016). Persistent Persister Misperceptions. *Frontiers in Microbiology*, *7*, 2134. https://doi.org/10.3389/fmicb.2016.02134

King, T., & Ferenci, T. (2005). Divergent roles of RpoS in *Escherichia coli* under aerobic and anaerobic conditions. *FEMS Microbiology Letters*, *244*(2), 323–327. https://doi.org/10.1016/j.femsle.2005.02.002

Kroll, J., Klinter, S., Schneider, C., Voß, I., & Steinbüchel, A. (2010). Plasmid addiction systems: perspectives and applications in biotechnology. *Microbial Biotechnology*, *3*(6), 634–657. https://doi.org/10.1111/j.1751-7915.2010.00170.x

Manav, M. C., Turnbull, K. J., Jurėnas, D., Garcia-Pino, A., Gerdes, K., & Brodersen, D. E. (2019). The *E. coli* HicB Antitoxin Contains a Structurally Stable Helix-Turn-Helix DNA Binding Domain. *Structure*, *27*(11), 1675-1685.e3. https://doi.org/10.1016/j.str.2019.08.008

Marcus, M. (2021). Going Beneath the Surface: Petroleum Pollution, Regulation, and Health. *American Economic Journal: Applied Economics*, *13*(1), 72–104.

Martinez, R., Flores, A. D., Dufault, M. E., & Wang, X. (2019). The XylR variant (R121C and P363S) releases arabinose-induced catabolite repression on xylose fermentation and enhances coutilization of lignocellulosic sugar mixtures. *Biotechnology and Bioengineering*, *116*(12), 3476–3481. https://doi.org/10.1002/bit.27144

Moelling, K., Broecker, F., Russo, G., & Sunagawa, S. (2017). RNase H As Gene Modifier, Driver of Evolution and Antiviral Defense. *Frontiers in Microbiology*, *8*, 1745. https://doi.org/10.3389/fmicb.2017.01745

Noh, M. H., Lim, H. G., Woo, S. H., Song, J., & Jung, G. Y. (2018). Production of itaconic acid from acetate by engineering acid-tolerant *Escherichia coli* W. *Biotechnology and Bioengineering*, *115*(3), 729–738. https://doi.org/10.1002/bit.26508

Novak, K., Flöckner, L., Erian, A. M., Freitag, P., Herwig, C., & Pflügl, S. (2018). Characterizing the effect of expression of an acetyl-CoA synthetase insensitive to acetylation on co-utilization of glucose and acetate in batch and continuous cultures of *E. coli* W. *Microbial Cell Factories*, *17*(1), 1–15. https://doi.org/10.1186/s12934-018-0955-2

Page, R., & Peti, W. (2016). Toxin-antitoxin systems in bacterial growth arrest and persistence. *Nature Chemical Biology*, *12*(4), 208–214. https://doi.org/10.1038/nchembio.2044

Park, J. H., Jang, Y. S., Lee, J. W., & Lee, S. Y. (2011). *Escherichia coli* W as a new platform strain for the enhanced production of L-Valine by systems metabolic engineering. *Biotechnology and Bioengineering*, *108*(5), 1140–1147. https://doi.org/10.1002/bit.23044

Park, S. H., Kim, H. U., Kim, T. Y., Park, J. S., Kim, S.-S., & Lee, S. Y. (2014). Metabolic engineering of Corynebacterium glutamicum for L-arginine production. *Nature Communications*. https://doi.org/10.1038/ncomms5618

Piao, X., Wang, L., Lin, B., Chen, H., Liu, W., & Tao, Y. (2019). Metabolic engineering of *Escherichia coli* for production of L-aspartate and its derivative β-alanine with high stoichiometric yield. *Metabolic Engineering*, *54*, 244–254. https://doi.org/10.1016/j.ymben.2019.04.012

Run, S., & Tian, P. (2018). Improved Tolerance of *Escherichia coli* to Propionic Acid by Overexpression of Sigma Factor RpoS. *Applied Biochemistry and Microbiology*, *54*(3), 288–293. https://doi.org/10.1134/S0003683818030122

Schellhorn, H. E. (2020). Function, Evolution, and Composition of the RpoS Regulon in *Escherichia coli. Frontiers in Microbiology*, *11*. https://doi.org/10.3389/fmicb.2020.560099

Sievert, C., Nieves, L. M., Panyon, L. A., Loeffler, T., Morris, C., Cartwright, R. A., Wang, X., & Demain, A. L. (2017). Experimental evolution reveals an effective avenue to release catabolite repression via mutations in XylR. *Proceedings of the National Academy of Sciences of the United States of America*, *114*(28), 7349–7354. https://doi.org/10.1073/pnas.1700345114

Song, S., & Wood, T. K. (2020). A Primary Physiological Role of Toxin/Antitoxin Systems Is Phage Inhibition. *Frontiers in Microbiology*, *11*. https://doi.org/10.3389/fmicb.2020.01895

Tsilibaris, V., Maenhaut-Michel, G., Mine, N., & Van Melderen, L. (2007). What is the benefit to *Escherichia coli* of having multiple toxin-antitoxin systems in its genome? *Journal of Bacteriology*, *189*(17), 6101–6108. https://doi.org/10.1128/JB.00527-07

Verstraeten, N., Knapen, W. J., Kint, C. I., Liebens, V., Van den Bergh, B., Dewachter, L., Michiels, J. E., Fu, Q., David, C. C., Fierro, A. C., Marchal, K., Beirlant, J., Versées, W., Hofkens, J., Jansen, M., Fauvart, M., & Michiels, J. (2015). Obg and Membrane Depolarization Are Part of a Microbial Bet-Hedging Strategy that Leads to Antibiotic Tolerance. *Molecular Cell*, *59*, 9–21. https://doi.org/10.1016/j.molcel.2015.05.011

Wang, X., Lord, D. M., Cheng, H. Y., Osbourne, D. O., Hong, S. H., Sanchez-Torres, V., Quiroga, C., Zheng, K., Herrmann, T., Peti, W., Benedik, M. J., Page, R., & Wood,

T. K. (2012). A new type V toxin-antitoxin system where mRNA for toxin GhoT is cleaved by antitoxin GhoS. *Nature Chemical Biology*, *8*(10), 855–861. https://doi.org/10.1038/nchembio.1062

Wang, X., Lord, D. M., Hong, S. H., Peti, W., Benedik, M. J., Page, R., & Wood, T. K. (2013). Type II toxin/antitoxin MqsR/MqsA controls type V toxin/antitoxin GhoT/GhoS. *Environmental Microbiology*, *15*(6), 1734–1744. https://doi.org/10.1111/1462-2920.12063

Wu, H., Liu, J., Miao, S., Zhao, Y., Zhu, H., Qiao, M., Erik Joakim Saris, P., & Qiao, J. (2018). Contribution of YthA, a PspC Family Transcriptional Regulator of Lactococcus lactis F44 Acid Tolerance and Nisin Yield: a Transcriptomic Approach. *Applied and Environmental Microbiology*, *84*(6), 1–20.

Yamaguchi, Y., & Inouye, M. (2011). Regulation of growth and death in *Escherichia coli* by toxin-antitoxin systems. *Nature Reviews Microbiology*, *9*(11), 779–790. https://doi.org/10.1038/nrmicro2651

Yamaguchi, Y., Park, J. H., & Inouye, M. (2011). Toxin-antitoxin systems in bacteria and archaea. *Annual Review of Genetics*, *45*, 61–79. https://doi.org/10.1146/annurev-genet-110410-132412

Zea, L., Larsen, M., Estante, F., Qvortrup, K., Moeller, R., de Oliveira, S. D., Stodieck, L., & Klaus, D. (2017). Phenotypic changes exhibited by *E. coli* cultured in space. *Frontiers in Microbiology*, *8*, 1–12. https://doi.org/10.3389/fmicb.2017.01598

Zhang, X., Wang, X., Shanmugam, K. T., & Ingram, L. O. (2011). L-malate production by metabolically engineered *Escherichia coli*. *Applied and Environmental Microbiology*, *77*(2), 427–434. https://doi.org/10.1128/AEM.01971-10

APPENDIX A

SUPPLEMENTARY FIGURES

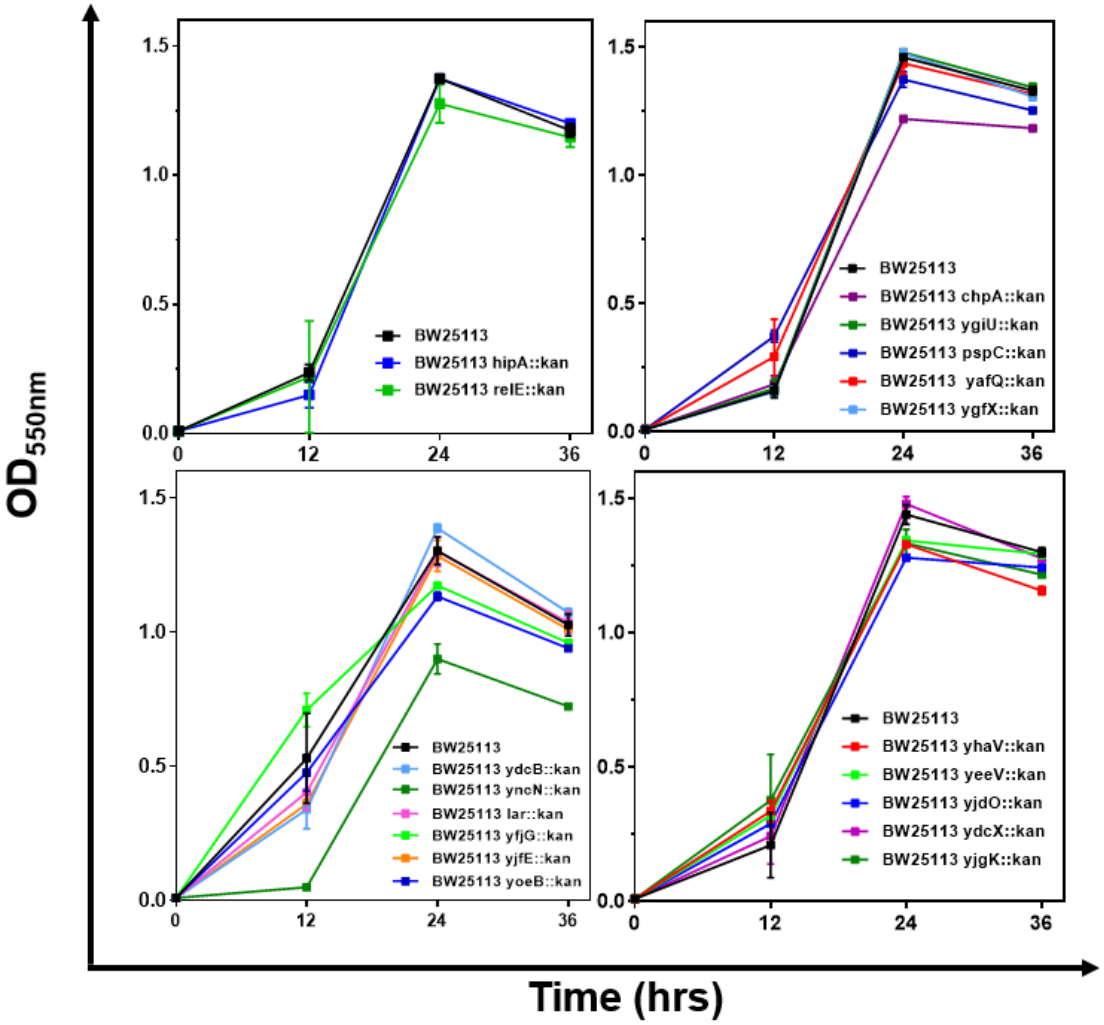

Figure S1. Growth curves of single toxin deletions in microaerobic conditions over 36 hours. Points are plotted as the average of at least two biological replicates. Growth curves look similar for all but the *yncN* knockout which performed significantly worse than the wild type.

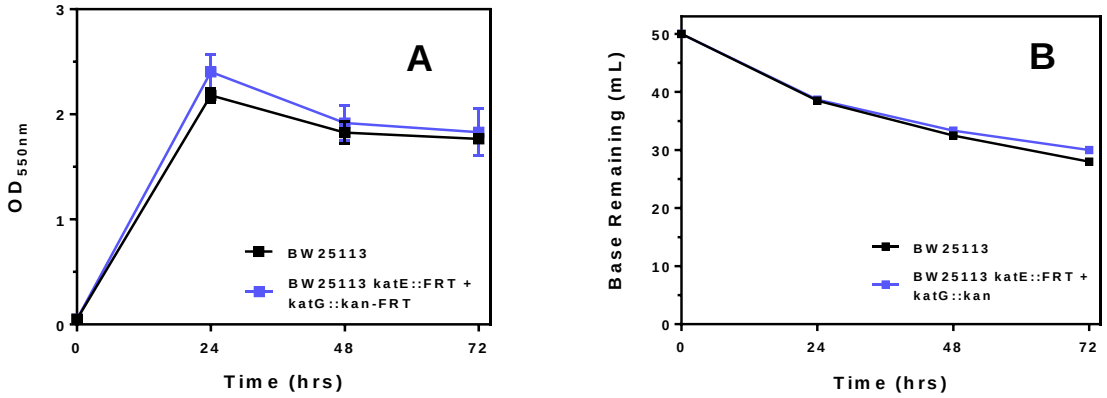

Figure S2. Fermentation of a *katE* and *katG* double knockout over 72 hours. (A) Points were plotted as the average of at least two biological replicates per strain. No significant changes in growth were observed in the double knockout strain. (B) All strains required ~18 mL of base to neutralize fermentation products with no significant variation between strains.

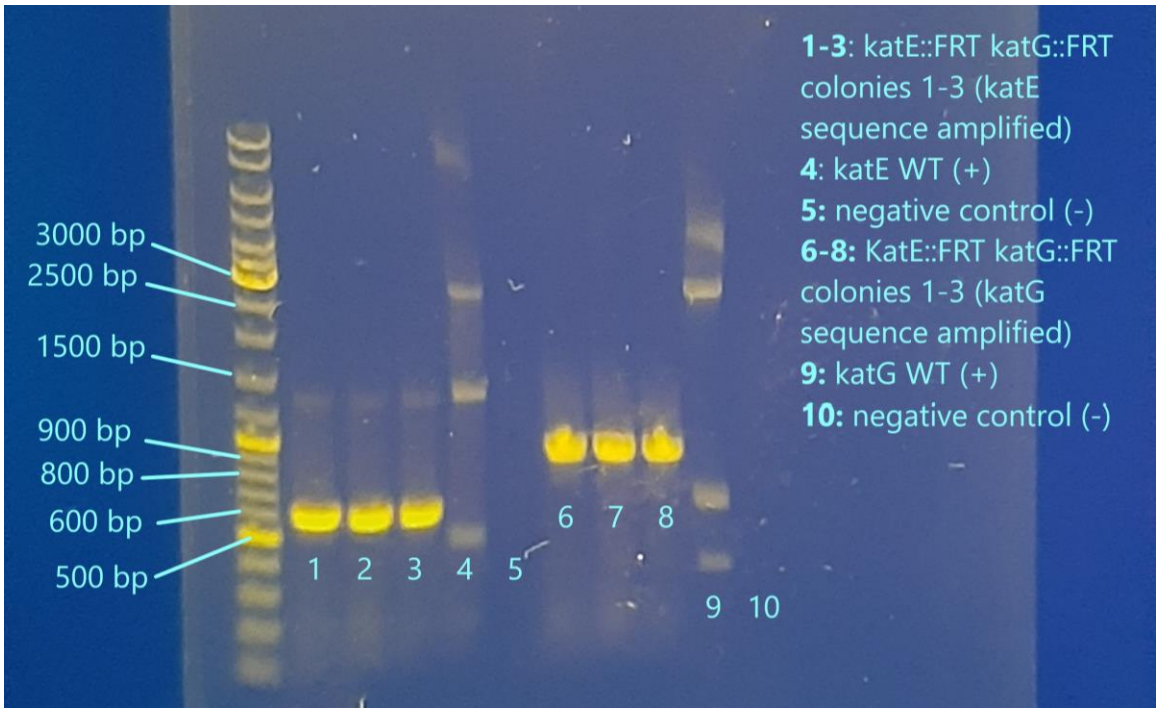

Figure S3. Agarose gel of colony PCR fragments in the construction of BW25113 *katE*::FRT, *katG*::kan. Lanes 1-3 show the amplified *katE* sequence after replacing it with an FRT site. Lane 4 shows the wild type *katE* sequence and lane 5 contains no DNA. Lanes 6-8 show the *katG* sequence after replacing it with a kanamycin resistance cassette. Lane 9 shows the amplified wild type *katG* sequence and lane 10 contains no DNA.

Table S1. List of primers used in this study

Primer	Sequence
katE-up	5' ataatctggcggttttgctg 3'
katE-down	5' tatcggttggggagttatcg 3'
katG-up	5' agccgtgaaggagtgaaaga 3'
katG-down	5' acggcatggtatagctcagg 3'

Table S2. List of strains used in this study

Strain name	**Name used in this study**	**Genotype**	**Source/Reference**
BW25113	BW25113	*rrnB3* DE*lacZ4787 hsdR514* DE(*araBAD*)*567* DE(*rhaBAD*)*568 rph-1*	Laboratory collection
JW5225-1	BW25113 *ydcB*::kan	F-, *Δ(araD-araB)567*, *ΔlacZ4787*(::rrnB-3), λ^-, *ΔhokB781::kan*, *rph-1*, *Δ(rhaD-rhaB)568*, *hsdR514*	(Baba et al., 2006)
JW5208-1	BW25113 *lar*::kan	F-, *Δ(araD-araB)567*, *ΔlacZ4787*(::rrnB-3), λ^-, *Δlar-785::kan*, *rph-1*, *Δ(rhaD-rhaB)568*, *hsdR514*	(Baba et al., 2006)
JW4184-2	BW25113 *yjfE*::kan	F-, *Δ(araD-araB)567*, *ΔlacZ4787*(::rrnB-3), λ^-, *rph-1*, *Δ(rhaD-rhaB)568*, *ΔchpB773::kan*, *hsdR514*	(Baba et al., 2006)
JW5230-2	BW25113 *yncN*::kan	F-, *Δ(araD-araB)567*, *ΔlacZ4787*(::rrnB-3), λ^-, *ΔyncN728::kan*, *rph-1*, *Δ(rhaD-rhaB)568*, *hsdR514*	(Baba et al., 2006)
JW3054-1	BW25113 *ygjN*::kan	F-, *Δ(araD-araB)567*, *ΔlacZ4787*(::rrnB-3), λ^-, *ΔygjN773::kan*, *rph-1*, *Δ(rhaD-rhaB)568*, *hsdR514*	(Baba et al., 2006)
JW1500-2	BW25113 *hipA*::kan	F-, *Δ(araD-araB)567*, *ΔlacZ4787*(::rrnB-3), λ^-, *ΔhipA728::kan*, *rph-1*, *Δ(rhaD-rhaB)568*, *hsdR514*	(Baba et al., 2006)
JW2753-1	BW25113 *chpA*::kan	F-, *Δ(araD-araB)567*, *ΔlacZ4787*(::rrnB-3), λ^-, *ΔchpA781::kan*, *rph-1*, *Δ(rhaD-rhaB)568*, *hsdR514*	(Baba et al., 2006)
JW2990-2	BW25113 *ygiU*::kan	F-, *Δ(araD-araB)567*, *ΔlacZ4787*(::rrnB-3), λ^-, *ΔmqsR720::kan*, *rph-1*, *Δ(rhaD-rhaB)568*, *hsdR514*	(Baba et al., 2006)
JW1299-1	BW25113 *pspC*::kan	F-, *Δ(araD-araB)567*, *ΔlacZ4787*(::rrnB-3), λ^-, *ΔpspC742::kan*, *rph-1*, *Δ(rhaD-rhaB)568*, *hsdR514*	(Baba et al., 2006)
JW2600-5	BW25113 *yfjG*::kan	F-, *Δ(araD-araB)567*, *ΔlacZ4787*(::rrnB-3), λ^-, *ΔyfjG775::kan*, *rph-1*, *Δ(rhaD-rhaB)568*, *hsdR514*	(Baba et al., 2006)
JW1555-2	BW25113 *relE*::kan	F-, *Δ(araD-araB)567*, *ΔlacZ4787*(::rrnB-3), λ^-, *ΔrelE785::kan*, *rph-1*, *Δ(rhaD-rhaB)568*, *hsdR514*	(Baba et al., 2006)
JW0215-1	BW25113 *yafQ*::kan	F-, Δ(*araD-araB*)*567*, *ΔyafQ743::kan*, *ΔlacZ4787*(::rrnB-3), *λ-*, *rph-1, Δ(rhaD-rhaB)568*, *hsdR514*	(Baba et al., 2006)

Table S2. Continued

Strain name	Name used in this study	Genotype	Source/Reference
JW3099-1	BW25113 *yhaV*::kan	F-, *Δ(araD-araB)567*, *ΔlacZ4787*(::rrnB-3), λ^-, *ΔyhaV744::kan*, *rph-1*, *Δ(rhaD-rhaB)568*, *hsdR514*	(Baba et al., 2006)
JW5331-1	BW25113 *yoeB*::kan	F-, *Δ(araD-araB)567*, *ΔlacZ4787*(::rrnB-3), λ^-, *ΔyoeB786::kan*, *rph-1*, *Δ(rhaD-rhaB)568*, *hsdR514*	(Baba et al., 2006)
JW1987-1	BW25113 *yeeV*::kan	F-, *Δ(araD-araB)567*, *ΔlacZ4787*(::rrnB-3), λ^-, *ΔyeeV773::kan*, *rph-1*, *Δ(rhaD-rhaB)568*, *hsdR514*	(Baba et al., 2006)
JW2864-1	BW25113 *ygfX*::kan	F-, *Δ(araD-araB)567*, *ΔlacZ4787*(::rrnB-3), λ^-, *ΔygfX747::kan*, *rph-1*, *Δ(rhaD-rhaB)568*, *hsdR514*	(Baba et al., 2006)
JW5732-2	BW25113 *yjdO*::kan	F-, *Δ(araD-araB)567*, *ΔlacZ4787*(::rrnB-3), λ^-, *rph-1*, *Δ(rhaD-rhaB)568*, *ΔyjdO755::kan*, *hsdR514*	(Baba et al., 2006)
JW5232-1	BW25113 *ydcX*::kan	F-, *Δ(araD-araB)567*, *ΔlacZ4787*(::rrnB-3), λ^-, *ΔydcX737::kan*, *rph-1*, *Δ(rhaD-rhaB)568*, *hsdR514*	(Baba et al., 2006)
JW5756-2	BW25113 *yjgK*::kan	F-, *Δ(araD-araB)567*, *ΔlacZ4787*(::rrnB-3), λ^-, *ΔydcX737::kan*, *rph-1*, *Δ(rhaD-rhaB)568*, *hsdR514*	(Baba et al., 2006)
JW1721-1	BW25113 *katE*::kan	F-, *Δ(araD-araB)567*, *ΔlacZ4787*(::rrnB-3), λ^-, *ΔkatE731::kan*, *rph-1*, *Δ(rhaD-rhaB)568*, *hsdR514*	(Baba et al., 2006)
JW3914-1	BW25113 *katG*::kan	F-, *Δ(araD-araB)567*, *ΔlacZ4787*(::rrnB-3), λ^-, *rph-1*, *Δ(rhaD-rhaB)568*, *ΔkatG729::kan*, *hsdR514*	(Baba et al., 2006)
BW25113 *katE*::FRT, *katG*::kan	BW25113 *katE*::FRT, *katG*::kan	F-, *Δ(araD-araB)567*, *ΔlacZ4787*(::rrnB-3), λ^-, *ΔkatE731::FRT*, *ΔkatG729::kan, rph-1*, *Δ(rhaD-rhaB)568*, *hsdR514*	This study